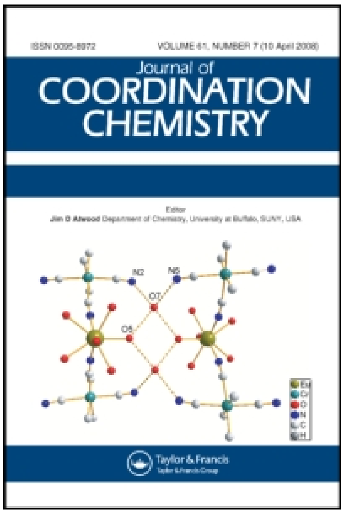

Journal of Coordination Chemistry
Publication details, including instructions for authors and subscription information:
http://www.informaworld.com/smpp/title~content=t713455674

Synthesis and spectral characterization of 1-(aminoformyl-<i>N</i>-phenylform)-4-ethylthiosemicarbazide and its metal complexes

O. A. El-Gammal[a]; A. A. El-Asmy[a]
[a] Faculty of Science, Chemistry Department, Mansoura University, Mansoura, Egypt

To cite this Article El-Gammal, O. A. and El-Asmy, A. A.(2008) 'Synthesis and spectral characterization of 1-(aminoformyl-<i>N</i>-phenylform)-4-ethylthiosemicarbazide and its metal complexes', Journal of Coordination Chemistry, 61: 14, 2296 — 2306

To link to this Article: DOI: 10.1080/00958970801907748

URL: http://dx.doi.org/10.1080/00958970801907748

Journal of Coordination Chemistry
Vol. 61, No. 14, 20 July 2008, 2296–2306

Taylor & Francis
Taylor & Francis Group

Synthesis and spectral characterization of 1-(aminoformyl-*N*-phenylform)-4-ethylthiosemicarbazide and its metal complexes

O. A. EL-GAMMAL and A. A. EL-ASMY*

Faculty of Science, Chemistry Department, Mansoura University, Mansoura, Egypt

(*Received 28 July 2007; in final form 15 October 2007*)

The chelating characteristics of 1-(aminoformyl-*N*-phenylform)-4-ethylthiosemicarbazide (H_3APET) towards Cr^{3+}, Fe^{3+}, Mn^{2+}, Co^{2+}, Ni^{2+}, Cu^{2+}, Cd^{2+}, Zn^{2+} and UO_2^{2+} ions have been investigated. The structures of the isolated complexes were assigned based on elemental and thermal analyses, spectra [IR, UV-visible, ^{1}H NMR, ESR (for Cu(II)) and mass] as well as magnetic measurements. The IR data reveal different coordination modes for H_3APET. Based on magnetic and spectroscopic studies Zn^{2+}, Fe^{3+}, Cd^{2+}, Ni^{2+}, UO_2^{2+} and Mn^{2+} complexes are octahedral, Co^{2+} and Cr^{3+} complexes are tetrahedral, while the Cu^{2+} complex is square-planar. Thermal stability and degradation kinetics of the complexes were studied by TGA and DTA and the kinetic parameters were evaluated.

Keywords: 1-(Aminoformyl-*N*-phenylform)-4-ethylthiosemicarbazide; Complexes; 1H NMR, ESR spectra; Thermal

1. Introduction

Interest in sulfur compounds arises from coordination ability, antimicrobial activity [1] and versatility in analytical chemistry [2–4]. Heterocyclic thiosemicarbazones and their metal complexes have been screened for antitumor activity [5]. Chelation in 4-ethyl- and 4-phenylthiosemicarbazides and their derivatives was found through the amine and thione groups [6–13]. Various applications on these compounds and their complexes were reported.

The present work focuses on synthesis, characterization and thermal behavior of a series of transition metal complexes of 1-(aminoformyl-*N*-phenylform)-4-ethylthiosemicarbazide (H_3APET) (Structure 1). The degradation kinetic parameters (n, E and A) and the other kinetic thermodynamic parameters (ΔG, ΔH and ΔS) have been evaluated [14–16]. Biological activity of the ligand and its metal complexes against gram positive and gram negative bacteria will be investigated.

---

*Corresponding author. Email: aelasmy@yahoo.com

Journal of Coordination Chemistry
ISSN 0095-8972 print/ISSN 1029-0389 online © 2008 Taylor & Francis
DOI: 10.1080/00958970801907748

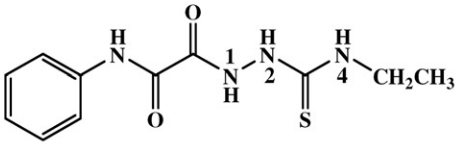

Structure 1. Keto-thione form of 1-(aminoformyl-N-phenylform)-4-ethylthiosemicarbazide.

2. Experimental

2.1. *Instrumentation and materials*

All chemicals were purchased from Aldrich and Fluka and used without further purification. Microanalyses were performed with a CHN Perkin-Elmer 2400 series II analyzer. Molar conductance values (10^{-3} mol L^{-1}) of the complexes in DMF were measured using a Tacussel conductivity bridge model CD6NG. Electronic spectra were recorded on a Unicam UV–Vis spectrophotometer UV_2. Magnetic susceptibilities were measured with a Sherwood Scientific magnetic susceptibility balance at 298 K. Infrared spectra (4000–400 cm^{-1}) as KBr discs were recorded on a Mattson 500 FTIR spectrometer. The ^{1}H NMR spectra at room temperature were measured on a Jeol JNMLA 300WB spectrometer at 400 MHz using TMS ($SiMe_4$) as internal standard. ESR spectra were obtained on a Bruker EMX spectrometer working in the X-band (9.78 GHz) with 100 kHz modulation frequency. The microwave power was set at 1 mW and modulation amplitude was set at 4 G. The low field signal was obtained after 4 scans with a 10 fold increase in receiver gain. A powder spectrum was obtained in a 2 mm quartz capillary at room temperature. Thermogravimetric measurements (TGA, DTA, 20–1000°C) were recorded on a DTG-50 Shimadzu thermogravimetric analyzer. The nitrogen flow and heating rate were 20 mL min^{-1} and 10°C min^{-1}, respectively.

2.2. *Synthesis of H_3APET*

2-Hydrazino-2-oxo-*N*-phenylacetamide ($PhNHCOCONHNH_2$) was synthesized according to the literature [17]. H_3APET (PhNHCOCONHNHCSNHEt, Structure 1) was synthesized by refluxing for 4 h in an ethanol solution of 2-hydrazino-2-oxo-*N*-phenylacetamide with ethylisothiocyanate. The white precipitate was filtered off, washed with ethanol and recrystallized from hot ethanol and finally dried in a vacuum desiccator over anhydrous $CaCl_2$ (m.p., 265–266°C; yield 90%; found: C: 49.48; H: 5.30; N: 20.92. Calcd: C, 49.61; H, 5.29; N, 20.03).

2.3. *Synthesis of metal complexes*

All complexes were prepared by refluxing 0.266 g (1.0 mmol) of H_3APET and 1.0 mmol of the hydrated metal salts (chloride or acetate) in 30 mL ethanol for 2–3 h. The solid complexes thus formed were filtered off, washed with ethanol several times followed by diethyl ether and dried in a vacuum desiccator over anhydrous $CaCl_2$. The physical and analytical data of H_3APET and its metal complexes are listed in table 1. The complexes did not decompose until 300°C and have high melting points, and are insoluble in common organic solvents (some are soluble in DMF and DMSO). The soluble complexes are non-electrolytes as indicated by molar conductivity values.

Table 1. Color, yield, melting point and elemental analysis of H_3EPTS and its complexes.

	Formula weight					Found (Calcd%)				
Compound/Formula	Found	Calcd	Color	Yield (%)	m.p. (°C)	M	Cl	C	H	N
H_3APET $C_{11}H_{14}N_4O_2S$	–	266.3	White	85	265–66	–	–	49.5 (49.6)	5.3 (5.3)	20.9 (21.0)
$[Cr(HAPET)Cl] \cdot H_2O$ $C_{11}H_{14}CrN_4O_3SCl$	369	369.9	Green	85	>300	14.4 (14.1)	9.2 (9.6)	35.5 (35.7)	4.7 (3.8)	15.1 (15.2)
$[Cu(H_2APET)Cl]$ $C_{11}H_{13}CuN_4O_2SCl$	327	327.7	Bright green	92	>300	19.0 (19.4)	–	40.1 (40.3)	3.7 (3.7)	17.0 (17.1)
$[Fe(HAPET)OH]$ $C_{11}H_{13}FeN_4O_3S$	328	329.2	Dark green	82	>300	16.6 (17.0)	–	40.8 (40.1)	3.7 (4.0)	12.5 (12.8)
$[Ni(H_3APET)Cl_2] \cdot 0.5H_2O$ $C_{11}H_{15}NiN_4O_3SCl_2$	403	405.0	Yellowish green	80	>300	14.1 (14.5)	17.0 (17.5)	33.0 (32.8)	3.7 (3.5)	13.1 (13.8)
$[UO_2(H_2APET)(OAc)] \cdot H_2O$ $C_{13}H_{16}UN_4O_6S$	–	592.4	Red	97	300	46.3 (46.3)	–	28.1 (28.4)	3.8 (2.8)	9.1 (9.5)
$[Co_2(H_3APET)Cl_4] \cdot 0.5H_2O$ $C_{11}H_{14}CoN_4O_3SCl_4$	534	535.0	Dark green	90	>300	22.4 (22.0)	25.9 (26.5)	25.0 (24.7)	3.9 (2.8)	10.2 (10.5)
$[Zn_2(HAPET)(OAc)_2(H_2O)_4] \cdot H_2O$ $C_{15}H_{28}Zn_2O_{11}N_4S$	604	603.2	White	80	>300	–	–	–	4.3 (4.7)	–
$[Cd(H_2APET)(OH)Cl]$ $C_{11}H_{14}CdN_4O_3SCl$	–	422.1	Yellow	82	>300	25.9 (26.6)	8.1 (8.4)	32.0 (31.3)	3.6 (3.3)	13.2 (13.3)
$[Mn_2(HAPET)(OAc)_2(H_2O)_4]$ $C_{15}H_{25}Mn_2N_4O_{10}S$	563	564.3	Dark brown	75	>300	19.2 (19.5)	–	31.7 (31.9)	4.1 (4.7)	9.3 (9.9)

Table 2. IR bands and their assignments for H_3EPTS and its complexes.

Compound	ν(NHPh)	ν(N^4HEt)	ν(N^1H)	N(N^2H)	ν(C=O)^1	ν(C=O)^2	ν(C=N*)	ν(C=S)	ν(M–O)
H_3APET	3314	3292	3171	3066	1716	1676	–	798	–
[Cr(HAPET)Cl] · H_2O	3338	3262	–	–	–	1625	1580	–	472
[Cu(H_2APET)Cl]	3432	3262	–	3074	–	1661	1622	755	502
[Fe(HAPET)(OH)]	3242	3222	–	–	–	1635	1601	–	570
[Ni(H_3APET)Cl_2] · 0.5H_2O	3343	3286	3169	3036	1632	1619	–	757	539
[UO_2(H_2APET)(OAc)] · H_2O	3313	3366	–	3313	–	1621	1621	754	–
[Co_2(H_3APET)Cl_4] · 0.5H_2O	3350	3277	3100	3042	1659	1620	–	756	516
[Zn_2(HAPET)$(OAc)_2(H_2O)_4$] · H_2O	3360	3285	–	3061	–	1663	1590	790	506

3. Results and discussion

3.1. *IR and ^{1}H NMR spectra*

The most important IR bands of H_3APET and its complexes are given in table 2. The ligand has numerous coordination sites and variable coordination modes. Its IR spectrum showed bands at 3313, 3287, 3188 and 3061 cm^{-1} assigned to ν(NHph), ν(N^4HEt), ν(N^1H) and ν(N^2H), respectively. Strong bands at 1716 and 1676 cm^{-1} are attributed to (C=O)^1 and (C=O)^2 while the medium intensity band at 950 cm^{-1} is ν(N–N) [18]. The 2970 and 2900 cm^{-1} bands are due to symmetric and asymmetric stretching vibrations of S–CH_2CH. No bands above 3350 or 2600–2500 cm^{-1} due to ν(OH) or ν(SH) suggest the thione-keto form (Structure 1). The ^{1}H NMR spectrum of H_3APET in d_6-DMSO showed signals at 8.16 (d, 1H), 9.33 (s, 1H) and 10.67 and 10.72 ppm (d, 2H) due to N^2H, N^1H, N^4HEt and NHph protons; the multiplets at 7.12–7.89 ppm are assigned to the protons of phenyl ring.

Comparison of the spectra of H_3APET and its complexes revealed that the ligand coordinates in the thione and thiol forms. In [Mn_2(HAPET)$(OAc)_2(H_2O)_4$] and [Zn_2(HAPET)$(OAc)_2(H_2O)_4$]H_2O, the ligand is binegative tetradentate coordinating through (C–O)^1, (C=O)^2, (C=N)* and (C–S) in the thiol-enol form. This mode of complexation is supported by: i) the disappearance of the bands due to ν(C=O)^1, ν(C=S), ν(N^2H) and ν(N^1H) with simultaneous appearance of new bands at 1164, 1567 and 655 cm^{-1} assigned to ν(C–O), ν(*N=C–C=N) and ν(C–S), respectively, ii) the shift of ν(C=O)^2 to 1562 and 1663 cm^{-1}, iii) new bands at 1562–1520 and 1411–1395 cm^{-1} indicating bidentate acetate [19] and iv) the appearance of new bands at 506 and 440 cm^{-1} assignable to ν(M–O) and ν(M–N) vibrations. Further evidence for deprotonation of the enolized carbonyl oxygen comes from the ^{1}H NMR spectrum of the diamagnetic Zn(II) complex, emphasizing the lack of the signals due to the (N^1H) and (N^2H) and the appearance of multiple signals at 3.57–3.41 ppm due to the CH_3CH_2 protons of the acetate.

The ligand is binegative tridentate, coordinating *via* (C–O)^2, (CN*) and (C–S) in [Cr(HAPET)Cl]H_2O and [Fe(HAPET)(OH)]. This is supported by the disappearance of ν(C=S), ν(C=O)^2, ν(N^1H) and ν(N^2H) vibrations, suggesting enolization of (C=O)^2 and thioenolization of (C=S) with the appearance of a band at 1635 cm^{-1} attributed to ν(CN*). Moreover, the spectrum of [Fe(HAPET)(OH)] showed a broad band at 3428 cm^{-1} due to ν(OH) covalently bonded to Fe.

The spectrum of [Ni(H_3APET)Cl_2] · ½H_2O showed a neutral tridentate ligand coordinating *via* (C=O)^1, (C=S) and (N^1H) by the shift of these bands to

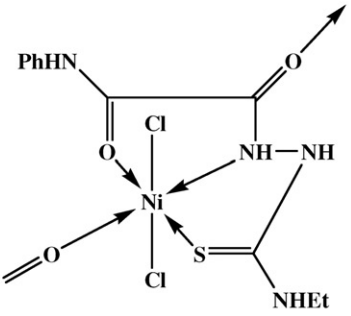

Structure 2. Structure of $[Ni(H_3APET)Cl_2] \cdot 0.5H_2O$.

1650, 752 and 3036 cm^{-1}. The $(C{=}O)^2$ band is affected due to chelation to another Ni. Steric factors prevent coordination of all donors in the ligand to a single metal ion, but the ligand may act as a bridge between the two metals through $(C{=}O)^2$, as shown in structure 2.

The IR spectrum of $[Co_2(H_3APET)Cl_4] \cdot ½H_2O$ revealed a neutral tetradentate ligand in which the coordination sites are $(C{=}O)^2$ and (N^1H) to one cobalt and (N^2H) and (C=S) to the other cobalt, as revealed by the shift of their bands to 3125, 3042 and 756 cm^{-1}, respectively (Structure 3).

In $[Cu(H_2APET)Cl]$ and $[Cd(H_2APET)Cl] \cdot ½H_2O$, the ligand is mononegative tridentate *via* $(C{=}O)^2$, $C{=}N^2$ and (C–S). This is suggested by the disappearance of $\nu(N^2H)$ and $\nu(C{=}S)$ with simultaneous appearance of bands at *ca* 1585 and 688–652 cm^{-1} attributed to $\nu(N{=}C)$ and $\nu(C–S)$. The two carbonyl bands are shifted to 1688–1661 and 1622–1616 cm^{-1}. Steric factors prevent coordination of the two carbonyl groups to a single metal ion, therefore, the ligand may bridge through $(C{=}O)^1$.

Finally, the IR spectrum of $[UO_2(HAPET)(OAc)]H_2O$ displayed bands at 932, 856 and 261 cm^{-1}, assigned to ν_3 and ν_1 vibrations, respectively, of the dioxouranium [20]. The ν_3 value was used to calculate the force constant (F) of (U=O) [14] by:

$$(\nu_3)^2 = \frac{(1307)^2(F_{U\text{–}O})}{14.103} \tag{1}$$

which was then substituted into the Jones relation [20]:

$$R_{U\text{–}O} = 1.08(F_{U\text{–}O})^{-1/3} + 1.17 \tag{2}$$

The calculated $F_{U\text{–}O}$ and $R_{U\text{–}O}$ were 7.171 mdynes Å^{-1} and 1.730 Å, respectively, falling within the usual range for uranyl complexes [21].

3.2. *Electronic spectra and magnetic moments*

The magnetic moments and significant electronic absorption bands of Cr^{+3}, Mn^{+2}, Fe^{+3}, Co^{+2}, Ni^{+2} and Cu^{+2} complexes, recorded in DMF or Nujul mull, are given in table 3 (DMF has no effect on the color). The electronic spectrum of the ligand showed $\pi \rightarrow \pi^*$ and $n \rightarrow \pi^*$ bands at 25380–28735 cm^{-1}. Large changes are observed for the

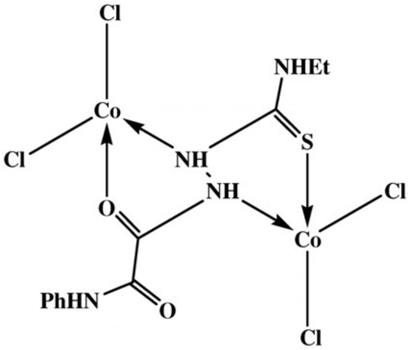

Structure 3. Structure of $[Co_2(H_3APET)Cl_4] \cdot 0.5H_2O$.

Table 3. Magnetic moments and electronic spectral bands of H_3EPTS and its complexes.

Complex	State	M_{eff} (B.M.)	d–d transition (cm^{-1})	Charge transfer bands (cm^{-1})
H_3APET	DMF	–	–	22625, 25680, 28735
$[Cr(HAPET)Cl] \cdot H_2O$	DMF	4.11	16665, 19840	26525, 25705, 24210
$[Cu(H_2APET)Cl]$	DMF	1.92	14165	24330, 27550, 30960
$[Fe(HAPET)(OH)]$	DMF	5.07	17360, 23040, 24690	25770, 21550
$[Ni(H_3APET)Cl_2] \cdot 0.5H_2O$	DMF	3.28	15625, 23695	25510, 27775, 22625
$[UO_2(H_2APET)(OAc)] \cdot H_2O$	DMF	–	24155	20700, 23865, 26245
$[Co_2(H_3APET)Cl_4] \cdot 0.5H_2O$	Nujol	1.98*	16555	28900, 25575, 24630
$[Mn_2(HAPET)(H_2O)_4(OAc)_2]$	Nujol	1.043*	17180, 14205	21550, 19305

*The value measured for one atom only.

Table 4. Decomposition steps and removing species of the complexes.

Complex	Temperature range (°C)	Species removed	Found (Calcd)%
$[Cu(H_2APET)Cl]$	247–307	$–C_8H_{12}N_2$	42.07 (41.55)
	308–388	$–(2CN+CO)$	24.78 (24.42)
	549–800	CuOS	33.06 (34.02)
$[Zn_2(HAPET)(H_2O)_4(OAc)_2] \cdot H_2O$	335–418	$–(5H_2O+C_4H_6O_4+CO+2CN)$	46.10 (47.62)
	419–657	$–C_8H_{13}N_2$	22.49 (22.67)
	658–800	ZnS+ZnO	29.12 (229.54)
$[UO_2(H_2APET)(OAc)] \cdot H_2O$	63–127	$–H_2O$	2.99 (2.09)
	128–306	$–C_2H_4O$	9.13 (9.96)
	307–412	$–(N_2+2CO+C_6H_6N)$	28.33 (29.90)
	414–516	$–C_2H_6N$	6.49 (7.44)
	517–800	UO_2CS	53.22 (53.09)
$[Co_2(H_3APET)Cl_4] \cdot 0.5H_2O$	38–90	$–0.5H_2O$	1.60 (1.69)
	91–266	stable	48.05 (47.98)
	267–486	$–(Cl_2+C_8H_{13}N_2)$	22.20 (21.12)
	487–660	$–(Cl_2+CS)$	22.20 (27.50)
	661–800	–2CoO	26.10 (27.50)
$[Mn_2(HAPET)(H_2O)_4(OAc)_2]$	152–198	$–H_2O$	3.2 (2.80)
	200–243	$–3H_2O$	9.60 (8.59)
	244–358	$–(C_4H_6O_4+C_8H_{10}N_2)$	44.05 (44.87)
	359–657	$–(N_2+CS+2C)$	16.09 (17.00)
	658–800	2MnO	24.94 (25.00)
$[Cd(H_2APET)(OH)Cl]$	145–233	$–(H_2O+Cl)$	10.24 (10.31)
	234–353	$–(CN+C_2H_6+2CO)$	48.38 (48.16)
	360–408	$–N_2$	6.62 (6.63)
	409–800	CdS	34.16 (34.23)

Table 5. Activation energy and thermodynamic parameters of some decomposition steps of the complexes using Coats-Redfern equation.

Complex	Stage	T (K)	E (kJ mol^{-1})	A (s^{-1})	ΔH (kJ mol^{-1})	ΔS (kJ mol^{-1} K)	ΔG (kJ mol^{-1})
[Cu(HEPTS)]	1st	534	276.92	1.08×10^{25}	272.47	0.2292	150.09
	2nd	609	338.78	9.76×10^{26}	333.72	0.2658	171.82
[Fe(HEPTS)OH]	1st	614.9	160.29	2.50×10^{11}	155.14	−0.0327	175.25
	2nd	761.6	142.65	1.87×10^{7}	136.32	−0.1135	222.69
	3rd	917.7	325.40	1.83×10^{16}	317.77	0.0571	265.36
$[Ni(H_3EPTS)Cl_2] \cdot 0.5H_2O$	1st	319.3	163.49	7.87×10^{24}	160.84	0.2311	87.04
	2nd	572.7	477.00	5.58×10^{41}	472.25	0.5472	158.86
	3rd	669.8	260.25	1.67×10^{18}	254.68	0.0972	189.55
$[UO_2(H_2EPTS)OAC] \cdot H_2O$	1st	316.8	298.25	5.44×10^{47}	295.61	0.6684	83.98
	4th	606.3	399.07	4.11×10^{32}	394.03	0.3735	175.03
$[Co_2(H_3EPTS)Cl_4] \cdot 0.5H_2O$	1st	665.7	77.98	5.64×10^{3}	72.45	−0.1798	192.07
	2nd	843.8	168.64	6.51×10^{7}	161.62	−0.1039	249.29
$[Cr(HEPTS)Cl] \cdot H_2O$	1st	624.7	227.57	7.04×10^{16}	222.38	0.0715	177.71
$[Mn_2(EPTS)(OAC)_2(H_2O)_4]$	1st	441.9	323.55	3.91×10^{36}	319.87	0.4523	120.14
	2nd	493.3	684.45	1.46×10^{71}	680.34	1.1133	131.29
	3rd	603.8	614.31	2.13×10^{25}	309.29	0.2341	168.00
	4th	641.9	597.47	1.59×10^{47}	592.13	0.6524	173.35
$[Cd(H_2EPTS)ClOH]$	1st	439.0	243.70	1.25×10^{27}	240.05	0.2706	121.26
	2nd	490.4	557.46	6.94×10^{57}	553.38	0.8583	132.47
	3rd	599.0	158.92	7.37×10^{11}	153.94	−0.0235	168.02
	4th	627.6	694.34	8.34×10^{55}	689.12	0.8195	174.86
$[Zn(H_2EPTS)_2] \cdot 0.5H_2O$	1st	662.8	387.98	5.14×10^{28}	382.47	0.2981	184.89
	2nd	725.7	260.25	1.67×10^{18}	254.21	0.0966	184.11
	3rd	853.3	818.86	1.43×10^{48}	811.77	0.6682	241.59

complexes with new $n \rightarrow \pi^*$ bands at 25510–30600 cm^{-1}. The band at 23040–24690 cm^{-1} in the spectra of the complexes may be due to LMCT. The electronic spectrum of $[Cr(HAPET)Cl]H_2O$ showed two strong absorption bands at 17480 (ν_2) and 19840 (ν_3) cm^{-1}, attributed to the $^4T_1(F) \rightarrow {}^4T_1(P)$ (ν_2) and $^4T_1(F) \rightarrow {}^4A_2(F)$ (ν_3) transitions in a tetrahedral geometry. An additional broad band centered at 24210 cm^{-1} is due to charge transfer. The ligand field parameters (Dq = 9350 cm^{-1}, B = 850 cm^{-1} and $\beta = 0.92$) are further support for the proposed geometry.

The electronic spectrum of $[Cu(H_2APET)Cl]$ exhibits two bands at 14185 and 27550 cm^{-1} assigned to $^2T_{2g} \rightarrow {}^2E_g$ and a symmetric forbidden ligand-metal charge transfer [22, 23]. The band position with the magnetic moment value (1.92 BM) is consistent with square planar geometry [24].

The magnetic moment value of $[Ni((H_3APET)Cl_2] \cdot ½H_2O$ of 3.28 BM is expected for octahedral structure with $^3A_{2g}$ ground term [25]. Its electronic spectrum showed broad bands centered at 23695 (ν_3) and 15625 cm^{-1} (ν_2) assigned to $^3A_{2g}(F) \rightarrow {}^3T_{1g}(P)$ (ν_3) and $^3A_{2g} \rightarrow {}^3T_{1g}(F)$ (ν_2) transitions [26, 27]. The spectral data give B (723 cm^{-1}), 10Dq (9487 cm^{-1}) and β and ν_1, $^3A_{2g} \rightarrow {}^3T_{2g}(F)$, to be 0.690 and 9487 cm^{-1}.

The electronic spectrum of $[Co_2(H_3APET)Cl_4] \cdot ½H_2O$, in Nujul mull, showed one band at 16556 cm^{-1} assigned to $^4A_2(F) \rightarrow {}^4T_1(F)$ (ν_3) characteristic for tetrahedral geometry. Bands at low frequency cannot be observed due to limitations of our equipment. The dark green color supports the proposed structure.

Table 6. Activation energy and thermodynamic parameters of some decomposition steps of the complexes using Horowitz–Metzger equation.

Complex	Stage	T (K)	E (kJ mol^{-1})	A (s^{-1})	ΔH (kJ mol^{-1})	ΔS (kJ mol^{-1} K)	ΔG (kJ mol^{-1})
[Cu(HEPTS)]	1st	534	276.59	2.21×10^{25}	272.16	0.2355	146.46
	2nd	609	339.06	2.21×10^{27}	333.99	0.2727	167.97
[Fe(HEPTS)OH]	1st	614.9	165.06	9.22×10^{11}	159.95	−0.0219	173.42
	2nd	761.6	148.53	7.90×10^{7}	142.19	−0.1015	219.43
	3rd	917.7	333.84	8.00×10^{16}	326.21	0.0693	662.61
$[Ni(H_3EPTS)Cl_2] \cdot 0.5H_2O$	1st	319.3	163.84	2.05×10^{25}	161.18	0.2391	84.84
	2nd	572.7	478.76	1.36×10^{42}	473.99	0.5563	155.42
	3rd	669.8	267.47	8.65×10^{18}	261.90	0.1108	187.63
$[UO_2(H_2EPTS)OAC] \cdot H_2O$	1st	316.8	299.39	1.39×10^{48}	296.76	0.6763	82.60
	4th	606.3	406.66	2.41×10^{33}	401.62	0.3883	174.74
$[Co_2(H_3EPTS)Cl_4] \cdot 0.5H_2O$	1st	665.7	90.78	5.45×10^{4}	85.25	−0.1609	192.40
	2nd	843.8	171.67	2.04×10^{5}	164.65	−0.0944	244.30
$[Cr(HEPTS)Cl] \cdot H_2O$	1st	624.7	229.90	1.98×10^{17}	224.71	0.0801	174.69
$[Mn_2(EPTS)(OAC)_2(H_2O)_4]$	1st	441.9	326.73	1.41×10^{37}	323.06	0.4629	118.46
	2nd	493.3	222.47	6.61×10^{21}	281.37	0.1686	235.49
	3rd	603.8	320.84	1.01×10^{26}	315.82	0.2470	166.68
	4th	641.9	611.10	1.59×10^{48}	605.77	0.6715	175.05
$[Cd(H_2EPTS)ClOH]$	1st	439.0	246.03	4.82×10^{27}	242.38	0.2818	118.67
	2nd	490.4	560.29	2.24×10^{58}	556.21	0.8679	131.03
	3rd	599.0	171.55	8.76×10^{12}	166.58	−0.0029	184.19
	4th	627.6	695.19	2.57×10^{56}	689.97	0.8288	169.82
$[Zn(H_2EPTS)_2] \cdot 0.5H_2O$	1st	662.8	395.81	2.83×10^{29}	390.29	0.3123	183.29
	2nd	725.7	202.28	2.80×10^{12}	196.25	−0.0140	206.41
	3rd	853.3	821.41	4.35×10^{48}	814.32	0.6775	236.21

The anomalous magnetic moment may be due to strong antiferromagnetic exchange between the two cobalt atoms.

The electronic spectrum of [Fe(HAPET)OH] exhibits multiple bands at 17361, 23041 and 24690 cm^{-1} assignable to $^6A_{1g} \rightarrow {}^4T_{1g}$, $^6A_{1g} \rightarrow {}^4E_g(G)$ and $^6A_{1g} \rightarrow {}^4T_{1g}(G)$, respectively. The magnetic moment (5.06 BM) is near the spin only value (5.87 BM) calculated for a d^5-system in a high spin octahedral geometry [28].

The low magnetic moment (1.04 BM) of $[Mn_2(HAPET)(OAc)_2(H_2O)_4]$ indicates a low spin octahedral complex. Its spectrum showed bands at 14204 and 17182 cm^{-1} due to $^6A_{1g} \rightarrow {}^4T_{1g}$ and M → L charge transfer. The deep brown color resembles $[Mn(CN)_6]^{4-}$, further evidence for low spin configuration [29].

Finally, the UV spectrum of $[UO_2(H_2APET)(OAc)] \cdot H_2O$ complex showed a band at 24691 cm^{-1} assigned to $^1\Sigma_g \rightarrow {}^3\pi_4$ similar to the OUO symmetric stretching frequency for the first excited state [30].

3.3. *Mass spectra*

The mass spectra recorded for most complexes and the molecular ion peaks confirmed the proposed formulae (table 1). As a typical example, the mass spectrum of $[Mn_2(HAPET)(OAc)_2(H_2O)_4]$ (supplementary material) showed peaks corresponding to the successive degradation of the molecule. The first peak at $m/e = 563$ represents

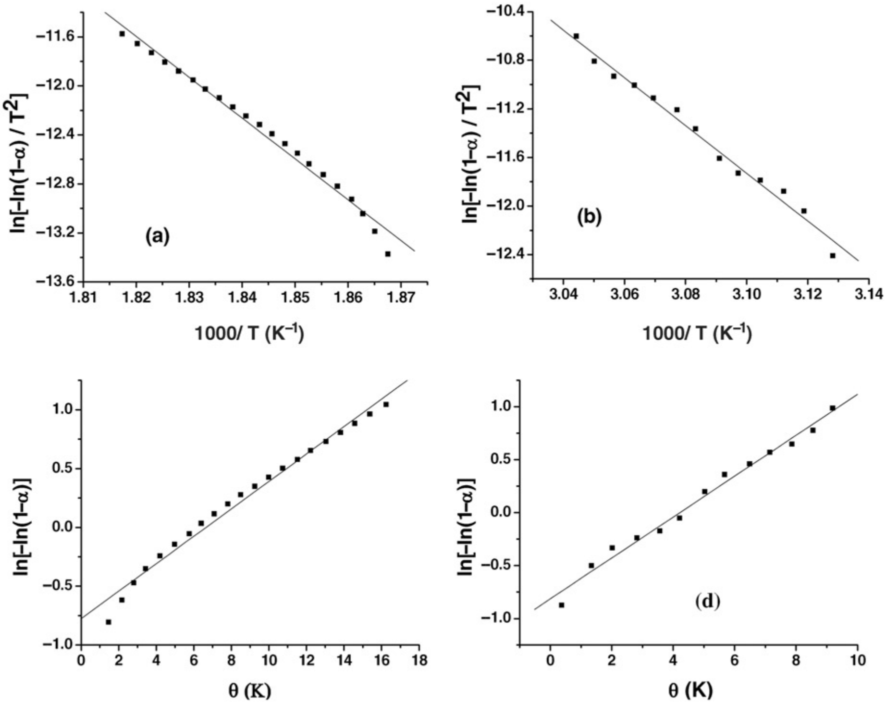

Figure 1. Coats-Redfern plots [*a* and *b*] and Horowitz-Metzger plots [*c* and *d*] of the first peak for [$Cu(H_2APET)Cl$] and [$Ni(H_3APET)Cl_2$] · $0.5H_2O$, respectively.

the molecular ion (Calcd = 564.3) with 3% abundance. The second sharp peak at $m/e = 369$ corresponds to the removal of $4 \cdot H_2O + 2 \cdot CH_3COO$. The peak at $m/e = 71$ with 64.15% abundance represents MnO.

3.4. *ESR spectra*

The spin Hamiltonian parameters and the G value of the solid Cu(II) complex ($S = 1/2$, $I = 3/2$) are calculated. The ESR spectrum of the complex displayed axially symmetric g-tensor parameters with $g_{\|} > g_{\perp} > 2.0023$ indicating that the copper site has a $d_{x^2-y^2}$ ground state characteristic of square-planar or octahedral geometry [31]. In axial symmetry, the g-values are related to the G-factor by $G = (g_{\|} - 2)/(g_{\perp} - 2)$; $G = 3.98$ indicates considerable exchange [32]. The ESR spectrum (supplementary material) showed $g_{\|}$ (2.24) > $g_{\perp}$ (2.06) > 2.0023 and $A_{\perp} = 175 \times 10^{-4}\,cm^{-1}$. A weak ESR absorption at 14140 G is consistent with square planar geometry [33, 34]. The molecular orbital coefficients α^2 (covalent in-plane σ-bonding) and β^2 (covalent in-plane π-bonding) were calculated to 0.78 and 0.73, respectively.

3.5. *Thermal analysis*

The stages of decomposition, temperature range, decomposition product as well as the found and calculated weight loss percentages of the complexes are given in table 4. In $[Ni((H_3APET)Cl_2] \cdot 0.5H_2O$, $[Co_2(H_3APET)Cl_4] \cdot 0.5H_2O$ and $[UO_2(H_2APET)(OAc)] \cdot H_2O$, the first decomposition at 23–127 represents elimination of water of hydration.

3.6. *Kinetic data*

In order to assess the influence of the structural properties of the ligand and the type of metal on the thermal behavior of the complexes, n and E of the various decomposition stages were determined using the Coats-Redfern [14] and Horowitz-Metzger [15] methods (tables 5 and 6 and figure 1). These results show:

(a) The high energies of activation (E) reveal the stability of such chelates [38].
(b) The positive sign of ΔG for the different decomposition steps indicates the decomposition steps are non-spontaneous.
(c) The negative ΔS values for Fe(III) and Co(II) complexes suggest more ordered activated complex than the reactants [39].

References

[1] D.W. West, S.B. Padhyde, P.B. Sonawane. *Structure and Bonding*, **76**, 1 (1991).
[2] H. Stunzi. *Aust. J. Chem.*, **35**, 1145 (1982).
[3] M.J.M. Campbell. *Coord. Chem. Rev.*, **5**, 279 (1973).
[4] S. Padhyde, G.B. Kauffman. *Coord. Chem. Rev.*, **63**, 127 (1985).
[5] M.C. Miller, K.F. Bastow, C.N. Stineman, J.R. Vance, S.C. Song, D.X. West, I.H. Hall. *Archiv der Pharmazie*, **331**, 121 (1998).
[6] S.E. Ghazy, M.A. Kabil, A.A. El-Asmy, Y.E. Sherief. *Afindad*, **456**, 128 (1995).
[7] A.A. El-Asmy, M.E. Khalifa, M.M. El-Defrawy, E.I. Asker, A.M. Abdellah. *Synth. React. Inorg. Met.-Org. Chem.*, **26**, 245 (1995).
[8] N.M. El-Metwally, R.M. El-Shazly, E. Gabr, A.A. El-Asmy. *Spectrochim. Acta A*, **61**, 1113 (2005).
[9] A.A. Abou-Hussen, I.M. Saad, A.A. El-Asmy. *J. Coord. Chem.*, **58**, 1735 (2005).
[10] N.M. El-Metwally, I.M. Gabr, A.M. Shallaby, A.A. El-Asmy. *J. Coord. Chem.*, **58**, 1154 (2005).
[11] N.M. El-Metwally, E.M. Gabr, A.A. Abou-Hussen, A.A. El-Asmy. *Transition Met. Chem.*, **31**, 71 (2006).
[12] G.M. Al-Hazmi, N.M. El-Metwally, O.A. El-Gammal, A.A. El-Asmy. *Spectrochim. Acta A*, in press (2007).
[13] I.S. Shehatta, A.A. El-Asmy, G.M. Abou El-Reash, F.I. Taha. *Bull. Electrochem*, **19**, 97 (2003).
[14] A.W. Coats, J.P. Redfern. *Nature*, **20**, 68 (1964).
[15] N. Oezpozan, H. Arslan, T. Oezpozan, N. Oezdes, N. Kueclue. *Thermochim. Acta*, **343**, 127 (2000).
[16] H.H. Horowitz, G. Metzger. *Anal. Chem.*, **25**, 1464 (1963).
[17] L.A. Cescon, A.R. Day. *J. Org. Chem.*, **27**, 581 (1962).
[18] D.N. Sathyanarayana, D. Nicholls. *Spectrochim. Acta A*, **34**, 263 (1978).
[19] K. Nakamoto. *Infrared Spectra of Inorganic and Coordination Compounds*, 3rd Edn, Wiley, New York (1970).
[20] L.H. Jones. *Spectrochim. Acta*, **10**, 395 (1958).
[21] S.P. McGlynn, J.K. Smith. *J. Chem. Phys*, **35**, 105 (1961).
[22] A. Syamal, K.S. Kale. *Indian J. Chem.*, **16A**, 46 (1978).
[23] A.K. Gregson, R.L. Martini, S. Mitra. *Proc. Roy. Soc.*, **320**, 473 (1971).
[24] L. Sacconi, M. Ciamolini. *J. Chem. Soc.*, 276 (1964).
[25] N.K. Singh, S.B. Singh. *Transition Met. Chem.*, **26**, 487 (2001).
[26] M. Palaniandavar, C.N. Natarajan. *Aust. J. Chem.*, **33**, 737 (1980).
[27] M.M. Mostafa, M.A. Khattab, K.M. Ibrahim. *Polyhedron*, **2**, 583 (1983).
[28] J.A. Bertrand, P.G. Eller. *Inorg. Chem.*, **13A**, 927 (1974).
[29] Y. Gultneh, Y.T. Tesema, B. Ahvazi, T.B. Yisgedu, R.J. Buther, J.P. Tuchagues. *Inorg. Chim. Acta*, **359**, 4463 (2006).
[30] S.P. McGlynn, J.K. Smith, W.C. Neely. *J. Mol. Spectrosc.*, **6**, 164 (1961).
[31] G. Speie, J. Csihony, A.M. Whalen, C.G. Piepont. *Inorg. Chem.*, **35**, 3519 (1996).

[32] B.J. Hathaway. *Struct. Bonding* (*Berlin*), **57**, 55 (1984).

[33] M.L. Miller, S.A. Ibrahim, M.L. Golden, M.Y. Daresboury. *Inorg. Chem.*, **42**, 2999 (1998).

[34] A. Diaz, A. Fragosa, R. Cao, V. Verez. *J. Carbohydrate Chem.*, **17**, 293 (1998).

[35] T. Taakeyama, F.X. Quinn. *Thermal Analysis Fundamentals and Applications to Polymer Science*, John Wiley and Sons, Chichester (1994).

[36] J.F. Mano, D. Koniarova, R.L. Reis. *J. Mater. Sci.: Mater. Medicine*, **14**, 127 (2003).

[37] A. Broido. *J. Polym. Sci.*, **7**, 1761 (1969).

[38] R.G. Mortimer. *Physical Chemistry: A. Harcourt and Science Technology Company*, Academic Press, San Diego (2000).

[39] A.A. Frost, R.G. Pearson. *Kinetics and Mechanisms*, Wiley, New York (1961).